

Total angular momentum conservation in *ab initio* Born-Oppenheimer molecular dynamicsXuezhi Bian ¹, Zhen Tao ^{1,*}, Yanze Wu ¹, Jonathan Rawlinson ², Robert G. Littlejohn,³ and Joseph E. Subotnik ^{1,†}¹*Department of Chemistry, University of Pennsylvania, Philadelphia, Pennsylvania 19104, USA*²*Department of Mathematics, University of Manchester, Manchester M13 9PL, United Kingdom*³*Department of Physics, University of California, Berkeley, California 94720, USA*

(Received 24 March 2023; revised 5 September 2023; accepted 29 November 2023; published 21 December 2023)

We prove both analytically and numerically that the total angular momentum of a molecular system undergoing adiabatic Born-Oppenheimer dynamics is conserved only when pseudomagnetic Berry forces are taken into account. This finding sheds light on the nature of Berry forces for molecular systems with spin-orbit coupling and highlights how *ab initio* Born-Oppenheimer molecular dynamics simulations can successfully capture the entanglement of spin and nuclear degrees of freedom as modulated by electronic interactions in the adiabatic limit.

DOI: [10.1103/PhysRevB.108.L220304](https://doi.org/10.1103/PhysRevB.108.L220304)

Introduction. Born-Oppenheimer (BO) theory [1,2] lies at the heart of two of the central problems in chemical physics—electronic structure theory and molecular dynamics. Under the Born-Oppenheimer theory, the total molecular wave function is separated into two components according to a mass difference: For the lighter electrons, one solves the electronic structure problems at different fixed nuclear geometries; for the slower nuclei, we simulate motion on a single (or sometimes on many coupled) electronic potential energy surface(s). As is well known by now [3,4], such a separation can lead to a nontrivial geometric phase and in general a gauge potential in the BO Hamiltonian [5].

Many intriguing phenomena have emerged from such a gauge structure. From the phase of an electronic eigenfunction transported around a conical intersection singularity, it is known [6–9] that a nuclear wave function will experience a sign change during cyclic motion. This molecular geometric phase effect is a topological effect and has been observed in various experiments [10,11].

Pseudoelectromagnetic fields also arise from the gauge structure in Born-Oppenheimer theory, leading to nontrivial interactions with the nuclear degrees of freedom (DOF) [12–15]. For the most part, the pseudoelectric contribution (i.e., the diagonal Born-Oppenheimer correction) is thought to be of less importance than the pseudomagnetic (i.e., Berry force) contribution [16]. Recently, experimental and theoretical developments in the solid state have suggested that such pseudomagnetic fields may lead to the phonon Hall effect [17–20] and the phonon contribution in the Einstein–de Haas effect [21]. In particular, the suggestion has been made that, in the presence of the pseudomagnetic gauge field, phonon modes can carry a nonzero angular momentum [22,23].

Although the notion of a chiral phonon carrying angular momentum induced by interactions with electronic and spin

degrees of freedom is becoming an active area of research nowadays [24,25], molecular analogs of such physics are not as well known and the relationship between the pseudomagnetic gauge field and nuclear angular momentum has not been fully explored [26–28]. The most important contributions so far have come from Li and co-workers, who used an exact factorization approach [29] to study angular momentum transfer between electrons and nuclei [30].

To understand the problem in detail, let us decompose the total angular momentum into its nuclear, electronic orbital, and electronic spin components (ignoring nuclear spin),

$$\mathbf{J}_{\text{tot}} = \mathbf{J}_{\text{nuc}} + \mathbf{J}_{\text{orb}} + \mathbf{J}_{\text{spin}}. \quad (1)$$

Due to the isotropy of space, the total angular momentum \mathbf{J}_{tot} must be conserved. However, neither \mathbf{J}_{nuc} nor \mathbf{J}_{ele} or \mathbf{J}_{spin} is a good quantum number; in principle, angular momentum can transfer between spins, electrons, and nuclei in the presence of spin-electronic-rovibrational couplings. The magnitudes of the fluctuations of these observable quantities is of interest, especially insofar as the possibility that spin polarization may emerge from nuclear motion, which is one possible explanation for the chirality-induced spin selectivity (CISS) effect [31–34].

With this background in mind, in what follows, we consider a radical molecular system with spin-orbit coupling (SOC). After reviewing the necessary equations of motion for propagating classical Born-Oppenheimer molecular dynamics (BOMD) with a pseudomagnetic gauge field, we analytically calculate the change in angular momentum. Note that, for a system with an odd number of electrons, electronic eigenstates arise in Kramers degenerate pairs according to time-reversal symmetry if we solve for the exact electronic eigenstates. We will assume that all dynamics follow one state in the Kramers degenerate set (which is equivalent to ignoring the off-diagonal component of the Berry curvature); this assumption represents an uncontrolled approximation, and yet running Hartree-Fock (HF) or density functional theory (DFT) Born-Oppenheimer dynamics is fairly standard nowa-

*taozhen@sas.upenn.edu

†subotnik@sas.upenn.edu

days, even in the case of a system with an odd number of electrons, given the cost of electronic structure calculations [35–46]. Within this Born-Oppenheimer assumption, we show that (unlike the linear momentum) the total angular momentum is conserved only if we include the pseudomagnetic gauge field that allows for angular momentum exchange between individual components. As a proof of concept, we perform real-time *ab initio* simulations for methoxy radical isomerization, an open-shell molecular system with SOC, and we identify the magnitudes of the relevant fluctuations in each individual component. We demonstrate that if we seek an *ab initio* framework for modeling spin dynamics in disordered environments, pseudomagnetic fields must be included within molecular dynamics simulations.

Born-Oppenheimer molecular dynamics. For a general molecular Hamiltonian $\hat{H} = \hat{T}_n + \hat{H}_{\text{el}}$ with spin-orbit coupling and electronic Hamiltonian

$$\hat{H}_{\text{el}} = \hat{T}_e + \hat{V}_{\text{ee}} + \hat{V}_{\text{en}} + \hat{V}_{\text{nm}} + \hat{V}_{\text{SO}}, \quad (2)$$

the total molecular wave function can be expressed as a sum of nuclear wave packets multiplied by adiabatic electronic basis functions

$$\Psi(\mathbf{R}, \mathbf{r}, s) = \sum_j \chi_j(\mathbf{R}) \Phi_j(\mathbf{r}, s; \mathbf{R}), \quad (3)$$

or for short

$$\langle \mathbf{r}, s | \Psi(\mathbf{R}) \rangle = \sum_j \chi_j(\mathbf{R}) \langle \mathbf{r}, s | \Phi_j(\mathbf{R}) \rangle. \quad (4)$$

Here, the adiabatic electronic wave functions $\{\Phi_j(\mathbf{r}, s; \mathbf{R})\}$ are functions of electronic position and spin; they are constructed as solutions to the time-independent electronic Schrödinger equation at fixed nuclear coordinate \mathbf{R} :

$$\hat{H}_{\text{el}}(\mathbf{R})|\Phi_j(\mathbf{R})\rangle = E_j(\mathbf{R})|\Phi_j(\mathbf{R})\rangle. \quad (5)$$

According to the Schrödinger equation, the nuclear wave packets are propagated as

$$i\hbar \frac{\partial}{\partial t} |\chi_j\rangle = \sum_k H_{jk}^{\text{BO}} |\chi_k\rangle \quad (6)$$

with the Born-Oppenheimer Hamiltonian,

$$\hat{H}_{jk}^{\text{BO}} = \sum_l \frac{(\hat{\mathbf{P}}\delta_{jl} - \mathbf{A}_{jl}) \cdot (\hat{\mathbf{P}}\delta_{lk} - \mathbf{A}_{lk})}{2M} + E_j \delta_{jk}. \quad (7)$$

Here, j, k label electronic eigenstates, $\hat{\mathbf{P}} = -i\hbar\nabla$ is the nuclear momentum operator, and $\mathbf{A}_{jk} = i\hbar\langle\Phi_j|\nabla|\Phi_k\rangle$ defines the Mead-Berry gauge potential. We will ignore the Born-Huang correction term here since these terms are usually small $\sim\hbar^2$ and do not contribute directly to the angular momentum.

Unfortunately, propagating coupled nuclear-electronic dynamics exactly is not possible for more than a few nuclear DOF in practice because of the computational demands. Approximations must be made [47–49]. One common approximation is to treat the nuclear DOF classically and keep the electronic DOF quantum mechanical which leads to a class of so-called “mixed-quantum-classical” methods [50,51] (e.g., the mean-field Ehrenfest [52,53] and fewest switches surface hopping algorithms [54–56]). An even simpler approach (that

we will take in this Letter) is to make the adiabatic approximation that the nuclei move slowly so that the system will stay on a single electronic eigenstate. In such a case, the effective Hamiltonian governing the system evolution simplifies to

$$\hat{H}_j^{\text{BO}} = \frac{(\hat{\mathbf{P}} - \mathbf{A}_{jj})^2}{2M} + E_j. \quad (8)$$

If we define the nuclear kinetic momentum operator by $\hat{\pi} = \hat{\mathbf{P}} - \mathbf{A}_{jj}$, note that one can derive the commutation relation,

$$[\hat{\pi}^{I\alpha}, \hat{\pi}^{J\beta}] = i\hbar\Omega_{jj}^{I\alpha J\beta}, \quad (9)$$

where the gauge-invariant Berry curvature tensor is defined as

$$\Omega_{jj}^{I\alpha J\beta} = (\nabla_{I\alpha} A_{jj}^{J\beta} - \nabla_{J\beta} A_{jj}^{I\alpha}). \quad (10)$$

Here, the index $I\alpha$ represents the Cartesian coordinate $\alpha = x, y, z$ of the I th atom. For adiabatic BO dynamics, a simple application of the Heisenberg equations of motion yields the following:

$$\frac{d\hat{R}^{I\alpha}}{dt} = \frac{i}{\hbar} [\hat{H}_j^{\text{BO}}, \hat{R}^{I\alpha}] = \frac{\hat{\pi}^{I\alpha}}{M^I}, \quad (11)$$

$$\begin{aligned} \frac{d\hat{\pi}^{I\alpha}}{dt} &= \frac{i}{\hbar} [\hat{H}_j^{\text{BO}}, \hat{\pi}^{I\alpha}] \\ &= -\nabla_{I\alpha} E_j + \frac{1}{2} \sum_{J,\beta} \left(\Omega_{jj}^{I\alpha J\beta} \frac{\hat{\pi}^{J\beta}}{M^J} + \frac{\hat{\pi}^{J\beta}}{M^J} \Omega_{jj}^{I\alpha J\beta} \right). \end{aligned} \quad (12)$$

According to Eq. (12), the force on a nuclear wave packet undergoing adiabatic motion can be separated into two parts: The first term is the usual BO force and the second term is the pseudomagnetic Berry force. At this point, if we also make the quantum-classical approximation, i.e., we replace all nuclear operators by their classical variables, it is straightforward to propagate molecular dynamics on a single BO energy surface provided we can compute the pseudomagnetic Berry force,

$$\mathbf{F}_{\text{Berry}}^{I\alpha} = \sum_{J,\beta} \Omega_{jj}^{I\alpha J\beta} \frac{\pi^{J\beta}}{M^J}. \quad (13)$$

Before focusing on the question of angular momentum conservation within this BO framework, however, several computational and theoretical details must be addressed.

First, Eqs. (11) and (12) are valid only in the adiabatic limit—which usually requires that BO energy surface E_j be well separated from all other surfaces (according to the Hellman-Feynman theorem). For the dynamics below, however, we will work in a regime where the nonadiabaticity is not overwhelming so that the adiabatic approximation is not terrible (see below).

Second, we have not yet discussed the key issues of electronic degeneracy or electronic structure, which are paramount when discussing Berry curvature for molecules. For a molecule with an odd number of electrons, Kramers’ theorem ensures the double degeneracy of all the electronic eigenstates over the entire nuclear configuration space. Even for a single eigenenergy, Eqs. (8)–(12) are not enough, and instead a non-Abelian SU(2) gauge theory must be considered [57,58],

$$H_{j,\mu\nu}^{\text{BO}} = \sum_{\eta} \frac{(\mathbf{P}\delta_{\mu\eta} - \mathbf{A}_{j\mu\eta}) \cdot (\mathbf{P}\delta_{\eta\nu} - \mathbf{A}_{j\eta\nu})}{2M} + E_j. \quad (14)$$

Here, the twofold degenerate eigenstates corresponding to the j th eigenenergy are indexed by μ and ν . The Hamiltonian described in Eq. (14) is gauge covariant, i.e., the nuclear dynamics are independent of the choice of gauge of electronic eigenstates. Now, generating electronic states in the case of degeneracy is difficult. For almost all *ab initio* dynamics calculations, one approximates the electronic eigenstate by a single Slater determinant (e.g., HF or DFT) as a compromise between accuracy and computation time. Below, we too model dynamics with a generalized Hartree-Fock (GHF) [59] (effectively a noncollinear DFT [60,61]) ansatz, where we include SOC. Of course, once the electronic structure packages generate one solution $|\mu\rangle$, we can also construct the corresponding time-reversed state $|\nu\rangle = \hat{T}|\mu\rangle$ (for time-reversible operator \hat{T}). In principle, one might imagine that these two states themselves are not unique, as one can always rotate together any two degenerate solutions and find another solution. That being said, the linear combination of any two such states will no longer be a single Slater determinant; thus if one propagates along a GHF+SOC solution, the electronic structure method effectively chooses a gauge frame for the user. Moreover, in the Supplemental Material (SM) [62], we show that, if we propagate the electronic wave function in the basis $\{|\mu\rangle, |\nu\rangle\}$, more than 98% of the resulting population still resides on state $|\mu\rangle$ after 120 fs and the fluctuations are weak. This empirical fact lends additional credence to our choice of running dynamics on one GHF state of a Kramer's pair (as mentioned above). We will show below (both analytically and computationally) that when we run dynamics along state $|\mu\rangle$, the total angular momentum is conserved if we include the pseudomagnetic Berry force.

Analytical treatment of angular momentum conservation. Within a BO representation for classical nuclei, the total linear momentum and angular momentum of a molecular system (moving along a single BO surface E_j with electronic eigenbasis $|\Phi_j\rangle$) are given by the sum of the classical and quantum expectation values:

$$\mathbf{P}_{\text{tot}} = \boldsymbol{\pi}_n + \langle \Phi_j(\mathbf{R}(t)) | \hat{\mathbf{P}}_e | \Phi_j(\mathbf{R}(t)) \rangle, \quad (15)$$

$$\mathbf{J}_{\text{tot}} = \mathbf{R}_n \times \boldsymbol{\pi}_n + \langle \Phi_j(\mathbf{R}(t)) | \hat{\mathbf{J}}_e | \Phi_j(\mathbf{R}(t)) \rangle. \quad (16)$$

In Eq. (15), we have written $\boldsymbol{\pi}_n = M\dot{\mathbf{R}}_n$ to represent the kinetic (as opposed to canonical) momentum of the nuclear DOF.

Now, BO theory requires wave-function gauge conventions [63], and for any electronic wave function, the most meaningful choice of gauge consistent with semiclassical theory satisfy translational and rotational invariance:

$$(\hat{\mathbf{P}}_e + \hat{\mathbf{P}}_n) | \Phi_j(\mathbf{R}(t)) \rangle = 0, \quad (17)$$

$$(\hat{\mathbf{J}}_n + \hat{\mathbf{J}}_e) | \Phi_j(\mathbf{R}(t)) \rangle = 0, \quad (18)$$

where $\hat{\mathbf{J}}_e = \hat{\mathbf{J}}_{\text{orb}} + \hat{\mathbf{J}}_{\text{spin}}$. Below, we will use Eqs. (17) and (18) to analyze momentum conservation, but in Sec. II of the SM [62], we will show that the same result can be obtained for any choice of smooth gauge.

From Eqs. (15) and (17), we can express the total linear momentum as

$$\sum_I \frac{dP_{\text{tot}}^{I\alpha}}{dt} = \sum_I \left(\frac{d\pi_n^{I\alpha}}{dt} - \frac{d\langle \Phi_j | \hat{P}_n^{I\alpha} | \Phi_j \rangle}{dt} \right) \quad (19)$$

$$= \sum_I \frac{d\pi_n^{I\alpha}}{dt} + \frac{dA_{jj}^{I\alpha}}{dt} \quad (20)$$

$$= \sum_I \frac{d\pi_n^{I\alpha}}{dt} + \frac{2}{\hbar} \sum_{I,J,k,\beta} \dot{R}_n^{J\beta} \text{Im}(A_{jk}^{I\alpha} A_{kj}^{J\beta}). \quad (21)$$

A similar expression can be derived for the total angular momentum using Eqs. (18) and (16):

$$\begin{aligned} \sum_I \frac{dJ_{\text{tot}}^{I\alpha}}{dt} &= \sum_I \left(\frac{dJ_n^{I\alpha}}{dt} - \frac{d\langle \Phi_j | \hat{J}_n^{I\alpha} | \Phi_j \rangle}{dt} \right) \\ &= \sum_I \frac{dJ_n^{I\alpha}}{dt} - \sum_{I,\beta,\gamma \neq \alpha} \epsilon_{\alpha\beta\gamma} R_n^{I\beta} \frac{d\langle \Phi_j | \hat{P}_n^{I\gamma} | \Phi_j \rangle}{dt} \\ &= \sum_I \frac{dJ_n^{I\alpha}}{dt} + \frac{2}{\hbar} \sum_{I,J,k,\delta, \beta,\gamma \neq \alpha} \epsilon_{\alpha\beta\gamma} R_n^{I\beta} \dot{R}_n^{J\delta} \text{Im}(A_{jk}^{I\gamma} A_{kj}^{J\delta}). \end{aligned} \quad (22)$$

We can now easily demonstrate that the total linear and angular momentum will be conserved for BO trajectories if and only if we use classical equations of motion that include the Berry force [and are consistent with Eqs. (11) and (12)]:

$$\frac{d\mathbf{R}_n}{dt} = \frac{\boldsymbol{\pi}_n}{M}, \quad (23)$$

$$\frac{d\boldsymbol{\pi}_n}{dt} = -\nabla E + \mathbf{F}_{\text{Berry}}. \quad (24)$$

Consider first the case of linear momentum: The right-hand side of Eq. (21) obviously vanishes if we plug in Eq. (24). At the same time, note that, in practice, we usually include electronic translation factors (ETFs) within electronic structure calculations [64–67] so that $\sum_I A_{kj}^{I\alpha} = 0$. Moreover, $\sum_I \dot{P}_n^{I\alpha} = 0$ whenever the BO forces in Eq. (24) arise from a Hamiltonian with translational invariance (as follows from Noether's theorem). Thus, there are effectively two ways to conserve linear momentum within a BO calculation: Either (i) one can properly calculate the Berry curvature dressed with ETFs, or (ii) one can work in a quick and dirty fashion, ignoring Berry curvature and equating canonical and kinetic momentum. In both cases, one will conclude that linear momentum is conserved.

Second, consider the case of angular momentum. Using Eqs. (23), (24), and the definition of \mathbf{J}_n in Eq. (16), it follows that $\dot{\mathbf{J}}_n = \mathbf{R}_n \times \mathbf{F}_{\text{Berry}}$ and therefore the right-hand side of Eq. (22) also clearly vanishes. Note that, unlike the case of linear momentum, angular momentum conservation can be achieved if and only if we include the Berry force in Eq. (24): The nuclear, electronic orbital, and electronic spin exchange angular momenta back and forth in a very complicated fashion that cannot be decomposed trivially as in the case of linear momentum.

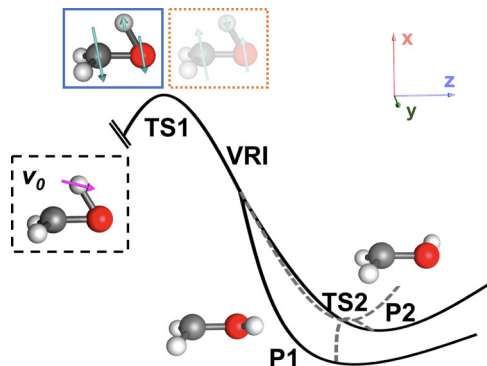


FIG. 1. A schematic figure of the methoxy radical isomerization reaction. The methoxy radical is initialized at TS1 with velocity \mathbf{V}_0 along the GHF-SOC solution with the majority spin down in the x direction (as illustrated by the blue box above TS1). The direction of \mathbf{V}_0 corresponds to the eigenvector with an imaginary eigenvalue of Hessian at TS1 and the initial kinetic energy is 0.006 kcal/mol. This system is known to have a bifurcation (VRI point) in the reaction pathway and two reaction channels P1 and P2 are possible.

Computational treatment of angular momentum conservation: Methoxy radical isomerization. As an example of the theory above, we have propagated BOMD on one of the ground doublet states of a methoxy radical. The potential energy surface is computed by GHF+SOC method with the 6-31G(d,p) basis set and we have included the one-electron Breit-Pauli form of the spin-orbit interaction. Details of the nuclear Berry force computation are given in SM [62]. The electronic structure was implemented in a local branch of Q-CHEM 6.0 [68]. The methoxy radical isomerization is interesting because of the presence of a valley-ridge inflection (VRI) point: The isomerization goes through one transition state (so-called TS1) and thereupon the reaction path bifurcates and allows for two different product wells (P1 and P2) [69]. For the post-transition state bifurcation simulations below, all methoxy radical dynamics were initiated at the transition state 1 (TS1) as computed via an unrestricted Hartree-Fock (UHF) calculation [70]. The trajectory was propagated with a step size of 2.5 a.u. (0.06 fs). The initial geometry and velocity are shown in Fig. 1. All dynamics are run along a single, smoothly varying GHF+SOC state (and there are, of course, two such states).

In Fig. 2, we plot the total angular momentum change as a function of time relative to time zero, $\langle \Delta J^\alpha \rangle = \langle J^\alpha(t) \rangle - \langle J^\alpha(0) \rangle$. We plot the individual nuclear, electronic, and spin components as calculated with (left-hand side) and without Berry force (right-hand side) as a function of time. As illustrated by Figs. 2(a), 2(c), and 2(e), the total angular momentum is conserved when including the Berry force. The change in nuclear angular momentum is nearly equal and opposite to the change in the spin angular momentum, while the electron orbital contribution is negligible. (For another trajectory, with non-negligible electronic orbital contributions, see Sec. VI of the SM [62].) In Figs. 2(b), 2(d), and 2(f), the results without Berry force show that the spin angular momentum changes are the same order of magnitude as in the case with Berry force, but the nuclear component is close to 0, so that there clearly is a violation of total angular momentum conservation.

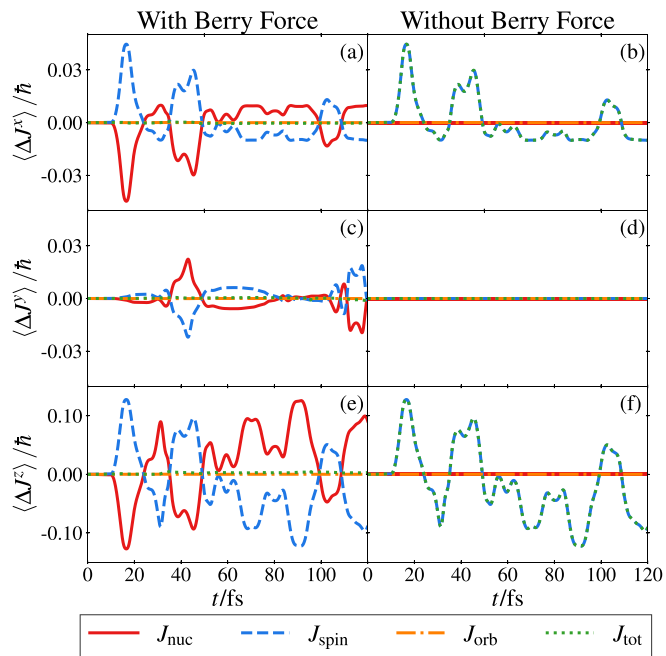


FIG. 2. The change in the real-time angular momentum $\langle \Delta J^\alpha(t) \rangle = \langle J^\alpha(t) \rangle - \langle J^\alpha(0) \rangle$ (relative to time zero) according to a BOMD trajectory of methoxy radical isomerization reaction with Berry force and without Berry force. For values at time zero, $J_{\text{spin}}^x = -0.49\hbar$, $J_{\text{spin}}^y = 0.00$, $J_{\text{spin}}^z = 0.10\hbar$, and $\mathbf{J}_{\text{nuc}} = \mathbf{J}_{\text{orb}} = 0$. (a), (c), and (e) correspond to the Cartesian coordinates x , y , and z shown in Fig. 1 [and the same for (b), (d), and (f)]. In (a), (c), and (e), with Berry force, the nuclei and spin transfer angular momentum among themselves, resulting in a conservation of total angular momentum. By contrast, without Berry force [as shown in (b), (d), and (f)], the total angular momentum is not conserved.

According to Figs. 2(a), 2(c), and 2(e), and Figs. 2(b), 2(d), and 2(f), when we include a Berry force, there is a clear transfer of angular momentum between electrons and spin and nuclei within the BO representation, while the total angular momentum is conserved. That being said, by comparing dynamics with and without Berry force, one does notice that the changes in spin angular momentum are small between the two calculations. In other words, there does not seem to be a large feedback mechanism; changing the nuclear dynamics by introducing a Berry force does not seem to induce large changes in spin for this particular set of dynamics. Whether these conclusions will hold more generally, however, is a very open question. For the present simulations, the spin-orbit coupling is small ($< 10^{-4}$ a.u.), we do not allow for nonadiabatic transitions, and there are few nuclear degrees of freedom. Previous work suggests that with more reaction channels available, the presence of many electronic states with the possibilities of conical intersections [71], and larger spin-orbit coupling, the feedback between nuclear and spin dynamics may well be larger. For this reason, the Berry force has recently attracted attention as a possible factor in CISS experiments.

In conclusion, we have used *ab initio* BOMD to illustrate that conserving total angular momentum requires including the pseudomagnetic Berry force. For a trajectory simulating methoxy radical isomerization, under the assumption that we

move along a single state of a Kramers doublet pair, including Berry force maintains angular momentum conservation, whereas without Berry force, the total angular momentum fluctuates.

The present results (for a system with an odd number of electrons) are relevant for systems with an even number of electrons as well. In such a case, indeed the true electronic ground state wave function must be real valued due to time-reversal symmetry [72], and hence the on-diagonal Berry curvature must be zero. However, approximate electronic structure methods such as GHF or noncollinear DFT with spin-orbit coupling often break time-reversal symmetry and yield complex-valued electronic states with nonzero Berry curvatures [73,74]; and recent work has demonstrated that, for such cases, the nonzero Berry curvature (as calculated by an approximate mean-field Schrödinger equation) can be meaningful [75]. In particular, in Ref. [75], we showed scattering results for which semiclassical calculations using an inexact mean-field electronic structure treatment plus a Berry force yielded better results than a calculation using an exact electronic structure treatment without a Berry force. Thus, in

general, simulations of coupled spin-nuclear dynamics (with even or odd numbers of electrons) must include angular momentum correctly if one seeks either to model spin-lattice relaxation [76,77] or to design and control spin-dependent chemical reactions with spin DOF [78].

Looking forward, new, rigorous quantum and semiclassical nonadiabatic frameworks will be crucial as far as going beyond the single-state approximation presented here and allowing us to disentangle how angular momentum is spread across multiple nuclear degrees of freedom and multiple electronic states (rather than just requiring that all motion occur along a single electronic state as we enforced here) [79,80]. Moreover, the effect of a Berry force may extend far beyond angular momentum conservation and have an impact on modeling chirality-induced spin separation [81] and avian bird magnetic field reception [82]. This field of entangled dynamics remains an exciting area of research at the intersection of spintronics, magnetochemistry, molecular dynamics, and light-matter physics for future development.

Acknowledgment. This work is supported by the National Science Foundation under Grant No. CHE-2102402.

-
- [1] M. Born and R. Oppenheimer, Zur Quantentheorie der Molekeln, *Ann. Phys.* **389**, 457 (1927).
- [2] M. Born, K. Huang, and M. Lax, Dynamical theory of crystal lattices, *Am. J. Phys.* **23**, 474 (1955).
- [3] C. A. Mead and D. G. Truhlar, On the determination of Born-Oppenheimer nuclear motion wave functions including complications due to conical intersections and identical nuclei, *J. Chem. Phys.* **70**, 2284 (1979).
- [4] M. V. Berry, Quantal phase factors accompanying adiabatic changes, *Proc. R. Soc. London, Ser. A* **392**, 45 (1984).
- [5] A. Böhm, A. Mostafazadeh, H. Koizumi, Q. Niu, and J. Zwanziger, *The Geometric Phase in Quantum Systems: Foundations, Mathematical Concepts, and Applications in Molecular and Condensed Matter Physics* (Springer, Berlin, 2003).
- [6] C. A. Mead, The geometric phase in molecular systems, *Rev. Mod. Phys.* **64**, 51 (1992).
- [7] B. Kendrick, Geometric phase effects in the vibrational spectrum of $\text{Na}_3(X)$, *Phys. Rev. Lett.* **79**, 2431 (1997).
- [8] B. K. Kendrick, Geometric phase effects in chemical reaction dynamics and molecular spectra, *J. Phys. Chem. A* **107**, 6739 (2003).
- [9] R. Requist, F. Tandetzky, and E. K. U. Gross, Molecular geometric phase from the exact electron-nuclear factorization, *Phys. Rev. A* **93**, 042108 (2016).
- [10] L. Schnieder, K. Seekamp-Rahn, J. Borkowski, E. Wrede, K. Welge, F. J. Aoiz, L. Bañiáres, M. D’mello, V. J. Herrero, V. S. Rabanos, and others, Experimental studies and theoretical predictions for the $\text{H} + \text{D}_2 \rightarrow \text{HD} + \text{D}$ reaction, *Science* **269**, 207 (1995).
- [11] D. Yuan, Y. Guan, W. Chen, H. Zhao, S. Yu, C. Luo, Y. Tan, T. Xie, X. Wang, Z. Sun, and others, Observation of the geometric phase effect in the $\text{H} + \text{HD} \rightarrow \text{H}_2 + \text{D}$ reaction, *Science* **362**, 1289 (2018).
- [12] M. V. Berry and J. Robbins, Chaotic classical and half-classical adiabatic reactions: Geometric magnetism and deterministic friction, *Proc. R. Soc. London, Ser. A* **442**, 659 (1993).
- [13] V. Krishna, Path integral formulation for quantum nonadiabatic dynamics and the mixed quantum classical limit, *J. Chem. Phys.* **126**, 134107 (2007).
- [14] M. Kolodrubetz, D. Sels, P. Mehta, and A. Polkovnikov, Geometry and non-adiabatic response in quantum and classical systems, *Phys. Rep.* **697**, 1 (2017).
- [15] R. Martinazzo and I. Burghardt, Quantum dynamics with electronic friction, *Phys. Rev. Lett.* **128**, 206002 (2022).
- [16] J. C. Tully, Perspective on “Zur Quantentheorie der Molekeln”, *Theor. Chem. Acc.* **103**, 173 (2000).
- [17] C. Strohm, G. L. J. A. Rikken, and P. Wyder, Phenomenological evidence for the phonon Hall effect, *Phys. Rev. Lett.* **95**, 155901 (2005).
- [18] L. Zhang, J. Ren, J.-S. Wang, and B. Li, Topological nature of the phonon Hall effect, *Phys. Rev. Lett.* **105**, 225901 (2010).
- [19] T. Qin, J. Zhou, and J. Shi, Berry curvature and the phonon Hall effect, *Phys. Rev. B* **86**, 104305 (2012).
- [20] T. Saito, K. Misaki, H. Ishizuka, and N. Nagaosa, Berry phase of phonons and thermal Hall effect in nonmagnetic insulators, *Phys. Rev. Lett.* **123**, 255901 (2019).
- [21] L. Zhang and Q. Niu, Angular momentum of phonons and the Einstein-de Haas effect, *Phys. Rev. Lett.* **112**, 085503 (2014).
- [22] L. Zhang and Q. Niu, Chiral phonons at high-symmetry points in monolayer hexagonal lattices, *Phys. Rev. Lett.* **115**, 115502 (2015).
- [23] D. Saparov, B. Xiong, Y. Ren, and Q. Niu, Lattice dynamics with molecular Berry curvature: Chiral optical phonons, *Phys. Rev. B* **105**, 064303 (2022).
- [24] H. Zhu, J. Yi, M.-Y. Li, J. Xiao, L. Zhang, C.-W. Yang, R. A. Kaindl, L.-J. Li, Y. Wang, and X. Zhang, Observation of chiral phonons, *Science* **359**, 579 (2018).
- [25] H. Chen, W. Zhang, Q. Niu, and L. Zhang, Chiral phonons in two-dimensional materials, *2D Mater.* **6**, 012002 (2018).

- [26] D. A. Garanin and E. M. Chudnovsky, Angular momentum in spin-phonon processes, *Phys. Rev. B* **92**, 024421 (2015).
- [27] T. Tsatsoulis, C. Illg, M. Haag, B. Y. Mueller, L. Zhang, and M. Fahnle, Ultrafast demagnetization after femtosecond laser pulses: Transfer of angular momentum from the electronic system to magnetoelastic spin-phonon modes, *Phys. Rev. B* **93**, 134411 (2016).
- [28] J. Simoni and S. Sanvito, Conservation of angular momentum in ultrafast spin dynamics, *Phys. Rev. B* **105**, 104437 (2022).
- [29] A. Abedi, N. T. Maitra, and E. K. U. Gross, Exact factorization of the time-dependent electron-nuclear wave function, *Phys. Rev. Lett.* **105**, 123002 (2010).
- [30] C. Li, R. Requist, and E. K. U. Gross, Energy, momentum, and angular momentum transfer between electrons and nuclei, *Phys. Rev. Lett.* **128**, 113001 (2022).
- [31] R. Naaman and D. H. Waldeck, Chiral-induced spin selectivity effect, *J. Phys. Chem. Lett.* **3**, 2178 (2012).
- [32] R. Naaman, Y. Paltiel, and D. H. Waldeck, Chiral molecules and the electron spin, *Nat. Rev. Chem.* **3**, 250 (2019).
- [33] T. K. Das, F. Tassinari, R. Naaman, and J. Fransson, Temperature-dependent chiral-induced spin selectivity effect: Experiments and theory, *J. Phys. Chem. C* **126**, 3257 (2022).
- [34] J. Fransson, Chiral phonon induced spin polarization, *Phys. Rev. Res.* **5**, L022039 (2023).
- [35] L. Noodleman, Valence bond description of antiferromagnetic coupling in transition metal dimers, *J. Chem. Phys.* **74**, 5737 (1981).
- [36] S. Hammes-Schiffer and H. C. Andersen, *Ab initio* and semiempirical methods for molecular dynamics simulations based on general Hartree-Fock theory, *J. Chem. Phys.* **99**, 523 (1993).
- [37] V. P. Antropov, M. I. Katsnelson, M. van Schilfgarde, and B. N. Harmon, *Ab initio* spin dynamics in magnets, *Phys. Rev. Lett.* **75**, 729 (1995).
- [38] M. Catti, *Ab initio* study of Li^+ diffusion paths in the monoclinic $\text{Li}_{0.5}\text{CoO}_2$ intercalate, *Phys. Rev. B* **61**, 1795 (2000).
- [39] D. Hobbs, G. Kresse, and J. Hafner, Fully unconstrained noncollinear magnetism within the projector augmented-wave method, *Phys. Rev. B* **62**, 11556 (2000).
- [40] R. Armunanto, C. F. Schwenk, A. B. Setiaji, and B. M. Rode, Classical and QM/MM molecular dynamics simulations of Co^{2+} in water, *Chem. Phys.* **295**, 63 (2003).
- [41] J. Kästner, S. Hemmen, and P. E. Blöchl, Activation and protonation of dinitrogen at the FeMo cofactor of nitrogenase, *J. Chem. Phys.* **123**, 074306 (2005).
- [42] H. Nakata, D. G. Fedorov, T. Nagata, S. Yokojima, K. Ogata, K. Kitaura, and S. Nakamura, Unrestricted Hartree-Fock based on the fragment molecular orbital method: Energy and its analytic gradient, *J. Chem. Phys.* **137**, 044110 (2012).
- [43] D. J. Vogel, T. M. Inerbaev, and D. S. Kilin, Role of lead vacancies for optoelectronic properties of lead-halide perovskites, *J. Phys. Chem. C* **122**, 5216 (2018).
- [44] I. Stockem, A. Bergman, A. Glensk, T. Hickel, F. Kormann, B. Grabowski, J. Neugebauer, and B. Alling, Anomalous phonon lifetime shortening in paramagnetic CrN caused by spin-lattice coupling: A combined spin and *ab initio* molecular dynamics study, *Phys. Rev. Lett.* **121**, 125902 (2018).
- [45] J. J. Goings, F. Egidi, and X. Li, Current development of non-collinear electronic structure theory, *Int. J. Quantum Chem.* **118**, e25398 (2018).
- [46] T. Culpitt, L. D. Peters, E. I. Tellgren, and T. Helgaker, *Ab initio* molecular dynamics with screened Lorentz forces. I. Calculation and atomic charge interpretation of Berry curvature, *J. Chem. Phys.* **155**, 024104 (2021).
- [47] D. F. Coker and L. Xiao, Methods for molecular dynamics with nonadiabatic transitions, *J. Chem. Phys.* **102**, 496 (1995).
- [48] B. F. Curchod and T. J. Martínez, *Ab initio* nonadiabatic quantum molecular dynamics, *Chem. Rev.* **118**, 3305 (2018).
- [49] T. R. Nelson, A. J. White, J. A. Bjorggaard, A. E. Sifain, Y. Zhang, B. Nebgen, S. Fernandez-Alberti, D. Mozyrsky, A. E. Roitberg, and S. Tretiak, Non-adiabatic excited-state molecular dynamics: Theory and applications for modeling photophysics in extended molecular materials, *Chem. Rev.* **120**, 2215 (2020).
- [50] R. Kapral and G. Ciccotti, Mixed quantum-classical dynamics, *J. Chem. Phys.* **110**, 8919 (1999).
- [51] R. Crespo-Otero and M. Barbatti, Recent advances and perspectives on nonadiabatic mixed quantum-classical dynamics, *Chem. Rev.* **118**, 7026 (2018).
- [52] P. Ehrenfest, Bemerkung über die angenäherte Gültigkeit der klassischen Mechanik innerhalb der Quantenmechanik, *Z. Phys.* **45**, 455 (1927).
- [53] H.-D. Meyer and W. H. Miller, A classical analog for electronic degrees of freedom in nonadiabatic collision processes, *J. Chem. Phys.* **70**, 3214 (1979).
- [54] J. C. Tully, Molecular dynamics with electronic transitions, *J. Chem. Phys.* **93**, 1061 (1990).
- [55] L. Wang, A. Akimov, and O. V. Prezhdo, Recent progress in surface hopping: 2011–2015, *J. Phys. Chem. Lett.* **7**, 2100 (2016).
- [56] J. E. Subotnik, A. Jain, B. Landry, A. Petit, W. Ouyang, and N. Bellonzi, Understanding the surface hopping view of electronic transitions and decoherence, *Annu. Rev. Phys. Chem.* **67**, 387 (2016).
- [57] C. A. Mead, Molecular Kramers degeneracy and non-Abelian adiabatic phase factors, *Phys. Rev. Lett.* **59**, 161 (1987).
- [58] H. Koizumi and S. Sugano, Geometric phase in two Kramers doublets molecular systems, *J. Chem. Phys.* **102**, 4472 (1995).
- [59] J. Kubler, K.-H. Hock, J. Sticht, and A. Williams, Density functional theory of non-collinear magnetism, *J. Phys. F: Met. Phys.* **18**, 469 (1988).
- [60] C. A. Jiménez-Hoyos, T. M. Henderson, and G. E. Scuseria, Generalized Hartree-Fock description of molecular dissociation, *J. Chem. Theory Comput.* **7**, 2667 (2011).
- [61] J. K. Desmarais, J.-P. Flament, and A. Erba, Spin-orbit coupling from a two-component self-consistent approach. I. Generalized Hartree-Fock theory, *J. Chem. Phys.* **151**, 074107 (2019).
- [62] See Supplemental Material at <http://link.aps.org/supplemental/10.1103/PhysRevB.108.L220304> for validation of single surface dynamics for the methoxy radical isomerization reaction; phase independence of linear and angular momentum conservation; details of computation of nuclear Berry curvature with GHF+SOC method; and another trajectory with non-negligible electronic orbital angular momentum contribution.
- [63] R. Littlejohn, J. Rawlinson, and J. Subotnik, Representation and conservation of angular momentum in the Born-Oppenheimer theory of polyatomic molecules, *J. Chem. Phys.* **158**, 104302 (2023).
- [64] S. Fatehi and J. E. Subotnik, Derivative couplings with built-in electron-translation factors: Application to benzene, *J. Phys. Chem. Lett.* **3**, 2039 (2012).

- [65] D. R. Bates and R. McCarroll, Electron capture in slow collisions, *Proc. R. Soc. London, Ser. A* **245**, 175 (1958).
- [66] J. B. Delos, Theory of electronic transitions in slow atomic collisions, *Rev. Mod. Phys.* **53**, 287 (1981).
- [67] C. Illescas and A. Riera, Classical outlook on the electron translation factor problem, *Phys. Rev. Lett.* **80**, 3029 (1998).
- [68] E. Epifanovsky, A. T. Gilbert, X. Feng, J. Lee, Y. Mao, N. Mardirossian, P. Pokhilko, A. F. White, M. P. Coons, A. L. Dempwolff, and others, Software for the frontiers of quantum chemistry: An overview of developments in the Q-Chem 5 package, *J. Chem. Phys.* **155**, 084801 (2021).
- [69] Z. Tao, T. Qiu, and J. E. Subotnik, Symmetric post-transition state bifurcation reactions with Berry pseudomagnetic fields, *J. Phys. Chem. Lett.* **14**, 770 (2023).
- [70] T. Taketsugu, N. Tajima, and K. Hirao, Approaches to bifurcating reaction path, *J. Chem. Phys.* **105**, 1933 (1996).
- [71] Y. Wu and J. E. Subotnik, Electronic spin separation induced by nuclear motion near conical intersections, *Nat. Commun.* **12**, 700 (2021).
- [72] C. A. Mead, The “noncrossing” rule for electronic potential energy surfaces: The role of time-reversal invariance, *J. Chem. Phys.* **70**, 2276 (1979).
- [73] O. Bistoni, F. Mauri, and M. Calandra, Intrinsic vibrational angular momentum from nonadiabatic effects in noncollinear magnetic molecules, *Phys. Rev. Lett.* **126**, 225703 (2021).
- [74] T. Culpitt, L. D. Peters, E. I. Tellgren, and T. Helgaker, Analytic calculation of the Berry curvature and diagonal Born-Oppenheimer correction for molecular systems in uniform magnetic fields, *J. Chem. Phys.* **156**, 044121 (2022).
- [75] X. Bian, T. Qiu, J. Chen, and J. E. Subotnik, On the meaning of Berry force for unrestricted systems treated with mean-field electronic structure, *J. Chem. Phys.* **156**, 234107 (2022).
- [76] D. Torchia and A. Szabo, Spin-lattice relaxation in solids, *J. Magn. Reson.* (1969) **49**, 107 (1982).
- [77] M. Hennecke, I. Radu, R. Abrudan, T. Kachel, K. Holldack, R. Mitzner, A. Tsukamoto, and S. Eisebitt, Angular momentum flow during ultrafast demagnetization of a ferrimagnet, *Phys. Rev. Lett.* **122**, 157202 (2019).
- [78] U. E. Steiner and T. Ulrich, Magnetic field effects in chemical kinetics and related phenomena, *Chem. Rev.* **89**, 51 (1989).
- [79] X. Bian, Y. Wu, H.-H. Teh, Z. Zhou, H.-T. Chen, and J. E. Subotnik, Modeling nonadiabatic dynamics with degenerate electronic states, intersystem crossing, and spin separation: A key goal for chemical physics, *J. Chem. Phys.* **154**, 110901 (2021).
- [80] X. Bian, Y. Wu, J. Rawlinson, R. G. Littlejohn, and J. E. Subotnik, Modeling spin-dependent nonadiabatic dynamics with electronic degeneracy: A phase-space surface-hopping method, *J. Phys. Chem. Lett.* **13**, 7398 (2022).
- [81] H.-H. Teh, W. Dou, and J. E. Subotnik, Spin polarization through a molecular junction based on nuclear Berry curvature effects, *Phys. Rev. B* **106**, 184302 (2022).
- [82] C. T. Rodgers and P. J. Hore, Chemical magnetoreception in birds: The radical pair mechanism, *Proc. Natl. Acad. Sci. USA* **106**, 353 (2009).